

Supplementary Information

Effective Degradation of Antibiotics by Near-infrared Excited Nonlinear Optical Heterojunctions through Atomic-level Regulation

Jianzhe Sun, Jiaqi Yu, Jing An, Minghao He, Yang Qu, and Guofeng Wang*

Key Laboratory of Functional Inorganic Material Chemistry Ministry of Education School of Chemistry and Materials Science, Heilongjiang University, Harbin 150080, P.R. China

* Corresponding author.

E-mail: wanguofeng@hlju.edu.cn (G. Wang)

1. Supplementary experimental section

Chemicals and Materials: Melamine ($C_3H_6N_6$, 99%, Aladdin), nitric acid solution, barium nitrate ($Ba(NO_3)_2$, 99%), thulium nitrate hexahydrate ($Tm(NO_3)_3 \cdot 6H_2O$, 99%), ytterbium (III) nitrate hexahydrate ($Yb(NO_3)_3 \cdot 6H_2O$, 99%), CTAB ($C_{19}H_{42}BrN$, 99%), cyclohexane (C_6H_{12} , 99.5%), 1-pentanol ($C_5H_{12}O$, 99%), hydrofluoric acid (HF, 40%), tetracycline ($C_{22}H_{24}N_2O_8$), ciprofloxacin ($C_{17}H_{18}FN_3O_3$). All reagents were of analytical grade and without further purification before utilization. Distilled water and ethanol were used in the whole experiments.

Synthesis of CN and CN:Tm (Tm single atom modified ultra-thin g- C_3N_4 nanosheets):

First, 5 g of melamine and a certain amount of Tm (NO_3)₃·6H₂O (0, 5, 25, 50 mg) were added to 30 mL of ethanol, stirred for 4 hours, and then dried in an oven. The powder was transferred to a covered crucible and was thermally polymerized in a Muffle furnace at 550 °C for 3 h at a rate of 2 °C/min. Then, the samples were cooled to room temperature naturally, and the yellowish bulk CN:Tm powder was obtained. 1 g of bulk CN:Tm was reheated to 550 °C for 2 h at a rate of 5 °C/min in an N₂ atmosphere. After the sample was cooled naturally, the yellow powder was added into a three-neck flask containing 100 ml 2M HNO₃ solution, and the reflux was conducted at 120 °C for 2 h. After centrifugation, the refluxed products were washed for five times with deionized water and ethanol until neutral. Finally, the ultra-thin g- C_3N_4 or g-

C₃N₄:Tm nanosheets were obtained by drying the obtained products. The samples were denoted as CN (ultra-thin g-C₃N₄ nanosheets) and CNT (ultra-thin g-C₃N₄:Tm nanosheets).

Synthesis of Ba₄Yb₃F₁₇:Tm (UC-x%Tm): Ba₄Yb₃F₁₇:Tm nanoparticles (UC particles) were prepared by the surfactant self-assembly method. In a typical procedure, CTAB (0.4 g) was dissolved in 6 mL of cyclohexane and 0.5 mL of 1-pentanol and stirred for 30 minutes until transparent, obtaining solution A. Different molar ratios of Ba(NO₃)₂, Yb(NO₃)₃·6H₂O, and Tm(NO₃)₃·6H₂O were dissolved in 25 mL deionized water to form a clear solution B. After stirring vigorously, the two microemulsion solutions were mixed and stirred for another 30 min, and 2 mL of 40% HF solution was added in the mixed solution. Then, the mixed solution was transferred into a 50 mL Teflon-lined stainless-steel autoclave and heated at 130 °C for 12 h. The resulting suspension was immediately cooled to room temperature. Then samples were washed several times with absolute ethanol and deionized water, centrifuged, and vacuum dried to obtain a white powder. Finally, the powder was calcined in air or N₂ atmosphere at different temperatures for 30 minutes. Here, the molar concentration of Yb³⁺ is fixed at 20% throughout the experiment, and the concentration of Tm was adjusted. Therefore, the name of the upconversion nanomaterial was named as UC-x%Tm.

Synthesis of g-C₃N₄:Tm@Ba₄Yb₃F₁₇:Tm (CNT/UC) composite photocatalyst: Taking the CNT/UC composite sample with a mass ratio of 1:6 for CNT:UC as an example, 0.4 g CTAB was dissolved in 6 mL of cyclohexane and 0.5 mL of 1-pentanol and stirred for 30 minutes until transparent, obtaining solution A. 0.795 mmol Ba(NO₃)₂, 0.2 mmol Yb(NO₃)₃·6H₂O, and 0.005 mmol Tm(NO₃)₃·6H₂O were dissolved in 25 mL deionized water to form a clear solution B. After stirring vigorously, the two microemulsion solutions were mixed and stirred for another 30 min, and 2 mL of 40% HF solution was added in the mixed solution. Then, a certain amount of CNT was added into the mixed solution and transferred into a 50 mL Teflon-lined stainless-steel autoclave and heated at 130 °C for 12 h. The resulting suspension was immediately cooled to room temperature. Then samples were washed several times with absolute ethanol and deionized water, centrifuged, and vacuum dried to obtain a light yellow powder. Finally, the powder was calcined in an air atmosphere at 500 °C for 30 minutes to obtain CNT/UC.

Material characterization: Powder X-ray diffraction (XRD) was collected on a Bruker D8 Advance diffractometer using Cu K α radiation ($\lambda=1.5406$ Å). Transmission electron microscopy (TEM) and elemental mapping were carried out on a JEM-2100 transmission

electron microscope using an accelerating voltage of 200 KV. Fourier transforms infrared (FTIR) spectra were measured on a Perkin-Elmer Spectrum One FTIR spectrometer using the KBr particle method. UV-Vis diffuse reflectance spectra (UV-DRS) of different solid powder samples were recorded on a SHIMADZU UV-2550 spectrophotometer in the wavelength range of 200-800 nm. In the photocatalytic degradation experiment, the concentration of organic pollutants was obtained using a UV-visible spectrophotometer (UV-1050, Techcomp). The N₂ adsorption and desorption isotherms (BET) were analyzed with Tristar II 3020. The pore size distribution charts were obtained by the Barrett-Joyner-Halenda (BJH) method. Photoluminescence (PL) spectra were measured using a Hitachi F-4600 spectrofluorophotometer equipped with a 150 W Xe lamp. Luminescence decay curves obtained were measured on FLSP920 Combined Stead State Fluorescence and Phosphorescence Lifetime Spectrometer ($\lambda_{\text{ex}} = 290 \text{ nm}$). X-ray photoelectron spectroscopy (XPS) analysis was performed on a Kratos-AXIS ULTRA DLD facility with an Al (single) X-ray source, using the binding energy of C 1 s at 284.8 eV as a reference. High Angle Annular Dark Field Image Scanning Transmission Electron Microscope (HAADF-STEM) images and sample images with atomic resolution were investigated using a JEM-ARM300F transmission electron microscope (TEM) equipped with a probe spherical aberration corrector. The up-conversion photoluminescence (UCPL) spectra of the samples were carried out using a Hitachi F-4600 spectrophotometer equipped with an external 980 nm IR fiber-coupled laser system. Scanning Kelvin Probe (SKP) was carried out at room temperature to evaluate the work function of the catalysts (SKP5050 system, Scotland).

Upconversion luminescence mechanism analysis: The NIR photons excite the Yb³⁺ ions in the Ba₄Yb₃F₁₇:Tm from the ground state (²F_{7/2}) to the excited state (²F_{5/2}). These excited Yb³⁺ ions act as sensitizers and populate higher energy levels of Tm³⁺ ions via the energy transfer process. By the successive energy transfer, the ³H₅, ³F_{2,3}, and ¹G₄ states of Tm³⁺ are activated leading to three transitions: ¹G₄→³H₆, ¹G₄→³F₄, and ³F_{2,3}→³H₆. The corresponding emissions are at 479 nm, 653 nm, and 701 nm, respectively. Two additional emissions at 364 and 455 nm correspond to the transitions from the ¹D₂ state to the ³H₆ and ³F₄ states, respectively. However, the ¹D₂ state could not be achieved by the excitation from the ¹G₄ state due to the large energy gap between them. There is the cross-relaxation process between the ³F₂ state and the ³H₄ state of two Tm³⁺ ions resulting in the populated ¹D₂ state. Subsequently, the ¹D₂ state would be excited to the ³P₂ state by the successive energy transfer from the Yb³⁺ ions. By the rapid

nonradiative relaxation, the 3P_1 , 3P_0 , and 1I_6 states are populated. The UV emission of 293 nm is further completed (from the 1I_6 state to the 3H_6 state).

Femtosecond transient absorption measurements: Femtosecond transient absorption (fs-TA) measurements were performed on a Helios (Ultrafast systems) spectrometers using a regeneratively amplified femtosecond Ti:sapphire laser system (Spitfire Pro-F1KXP, Spectra-Physics; frequency, 1 kHz; max pulse energy, ~ 8 mJ; pulse width, 120 fs) at room temperature. Finally, analyze the data through commercial software (Surface Xplorer, Ultrafast Systems).

Photoelectrochemistry property measurements: Photocurrent responses, electrochemistry impedance spectra (EIS), and Mott-Schottky curves were measured with a CHI660E electrochemical analyzer (Chenhua Instruments Co., Shanghai) in a three-electrode electrochemical system with a quartz window. A platinum electrode was used as an electrode, a saturated Ag/AgCl electrode as a reference electrode, and a photocatalyst was loaded on an FTO conducting glass as the working electrode. 0.5 mol/L Na_2SO_4 aqueous solution was used as the electrolyte for all measurements. For photocurrent response measurement, a 350 W Xe lamp served as the light source and the 940 nm bandpass filter was used to obtain the near-infrared (NIR) light. The applied potential window was -1.0~1.0 V, and the applied frequency was 1 kHz for the Mott-Schottky curve measurement. The working electrode was prepared as follows: under vigorous stirring, the prepared photocatalyst (0.1 g) was added to isopropanol (1 mL), and polyethylene glycol (0.05 g) was added for sonication for 20 min. Subsequently, the solution was further vigorously stirred for 30 minutes, to which acetylacetone (0.05 ml) was added, and the resulting solution was maintained under vigorous stirring for one week. 1 cm \times 1 cm conductive fluorine-doped tin oxide (FTO)-coated glass was used as the substrate, and the prepared slurry was coated on the substrate by a doctor blade method and finally dried at 80 $^\circ\text{C}$ for 12 h.

Photocatalytic performance evaluation: The degradation efficiency of TC and CF was used as the index to measure the photocatalytic performance of samples. In this work, a 300 W Xe lamp was used as light source, and the 940 nm bandpass filter was used to obtain the near-infrared (NIR) light. The high permeability quartz photochemical reactor is used to keep the temperature of the reaction system at a constant 20 $^\circ\text{C}$, with bidirectional circulating water entering through the lower hole and discharging through the upper hole. Typically, 50 mg photocatalyst was added to 50 mL TC or CF solution (20 mg/L). Prior to irradiation, the

suspension was magnetically stirred in the dark for 30 min to ensure the establishment of an adsorption/desorption equilibrium. Under simulated NIR light irradiation, a sample of 4mL mixture was taken at 30 minute intervals, and the concentration changes of TC and CF were measured after removing the catalyst by centrifugation. The concentration of TC and CF antibiotics was estimated by their absorption at 275 and 265 nm by a UV-visible spectrophotometer (UV-1050, Techcomp), respectively. The formula for calculating the photocatalytic degradation efficiency (η , %) of TC or CF is as follows: $\eta = (C_0 - C_t) / C_0 \times 100\%$. Where C_0 represents the initial TC or CF concentration, while C_t represents the TC or CF concentration after t min degradation. To measure the stability of the photocatalyst, the photodegradation reaction was carried out for four cycles, and the time of each photodegradation reaction was 2 hours.

Specific experimental details for LC-MS/MS technology: The intermediates produced and path by photocatalytic degradation of TC molecule were analyzed by LC-MS/MS (Ultimate 3000 UHPLC - Q Exactive, Thermo Scientific, US) with an Eclipse Plus C18 column (4.6×100 mm). The column temperature was 30 °C. The mobile phase was composed of 0.1% (v/v) formic acid (HCOOH) and acetonitrile (C₂H₃N) at a flow rate of 0.4 mL /min. The injection volume was 10 μ L. The linear gradient elution procedure is as follows: Initially, the volume ratio of formic acid in the mobile phase decreased gradually from 90% to 10% within 10 min and remained for 4 min. Subsequently, the volume of formic acid rose again to 90% within 2 min and maintained for 4 min. Electrospray ionization (ESI) source was used for MS analysis in positive ion mode, and specific conditions are as follows: the range of MS scanning, 50 to 600 m/z; Auxiliary gas (N₂) temperature, 300 °C; ion spray voltage, 3.8 kV.

Computational details for DFT calculations: The plane-wave ultrasoft (PWUS) pseudopotential method, as implemented in the Cambridge Sequential Total Energy Package (CASTEP) algorithm, was used to mimic all geometric optimizations, band structure, and the partial density of states (PDOS), work function, and charge density difference. The absorption spectra were obtained in CASTEP using the Perdew-Burke-Ernzerhof (PBE) functional. The generalized gradient approximation (GGA) with the PBE exchange-correlation functional was applied in the calculations. The plane-wave expansion's cutoff energy was set to 400 eV. The Brillouin zone integration was performed with $3 \times 4 \times 1$ k-points for geometry optimization. The criteria for convergence in the total energy, force, and displacement convergence threshold are 1.0×10^{-5} eV/atom, 0.05 eV/Å, and 0.005 Å, respectively. Geometry optimization, electronic

structure, and optical property calculations were all performed using spin-polarized magnetic computation.

X-ray absorption spectroscopy (XAFS) measurements. The XAFS study was performed at the BL14B2* of SPring-8 (8 GeV, 100 mA), Japan, in which, the X-ray beam was monochromatized with water-cooled Si (111) double-crystal monochromator and focused with two Rh coated focusing mirrors with the beam size of 2.0 mm in the horizontal direction and 0.5 mm in the vertical direction around sample position, to obtain X-ray adsorption fine structure (XAFS) spectra both in near and extended edge. Tm_2O_3 samples were used as references. However, although the Tm element content in the composite sample to be tested is 0.5%wt, the test results still show that the Tm signal is weak and the test effect is very poor. At the same time, if an oxide with similar energy (Tm_2O_3) is used as a standard sample, the results cannot be measured, making it impossible to reference and compare the samples during the data analysis process. Due to the characteristics of the Tm element, its position in the periodic table is closely linked to that of the Yb element. Affected by the Yb element, the Tm data overlaps with the Yb data, making the test results unreliable. On the other hand, as the amount of sample increases, the absorption coefficient beyond the absorption edge increases. When the amount of sample is too large ($\Delta\mu t > 4$), the X-ray do not pass through the sample beyond the absorption edge (Figure S18).

2. Supplementary texts, tables, and figures.

Table S1. Control experiments to prepare the upconversion nanoparticles (UCNPs) with different Tm^{3+} concentrations (the molar concentration of Yb^{3+} is fixed at 20%) calcined at 500 °C in air for 30 minutes. It is noted that the UC:0.5%Tm sample has the best UC luminescence performance, therefore, the UC:0.5%Tm was chosen to further prepare CN@UC and CN:Tm@UC composites. The abbreviations of the composite samples are shown in Table S5.

Samples	Ba(NO ₃) ₂ (mmol)	Yb(NO ₃) ₃ (mmol)	Tm(NO ₃) ₃ (mmol)	Hydrothermal condition	Calcined temperature
UC-0.1%Tm	0.799	0.2	0.001	130 °C, 12 h	500 °C
UC-0.3%Tm	0.797	0.2	0.003	130 °C, 12 h	500 °C
UC-0.5%Tm	0.795	0.2	0.005	130 °C, 12 h	500 °C
UC-1%Tm	0.79	0.2	0.01	130 °C, 12 h	500 °C
UC-2%Tm	0.78	0.2	0.02	130 °C, 12 h	500 °C

Table S2. Control experiments to prepare the UC-0.5%Tm calcined at different temperatures in air for 30 minutes.

Samples	Ba(NO ₃) ₂ (mmol)	Yb(NO ₃) ₃ (mmol)	Tm(NO ₃) ₃ (mmol)	Hydrothermal condition	Calcined temperature
UC-0.5%Tm	0.795	0.2	0.005	130 °C, 12 h	500 °C
	0.795	0.2	0.005	130 °C, 12 h	600 °C
	0.795	0.2	0.005	130 °C, 12 h	700 °C

Table S3. Control experiments to prepare the UC-0.5%Tm calcined at different temperatures in nitrogen for 30 minutes.

Samples	Ba(NO ₃) ₂ (mmol)	Yb(NO ₃) ₃ (mmol)	Tm(NO ₃) ₃ (mmol)	Hydrothermal condition	Calcined temperature
UC-0.5%Tm	0.795	0.2	0.005	130 °C, 12 h	500 °C
	0.795	0.2	0.005	130 °C, 12 h	600 °C
	0.795	0.2	0.005	130 °C, 12 h	700 °C

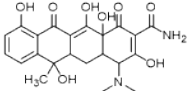
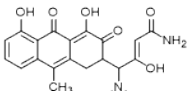
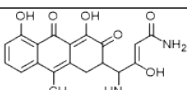
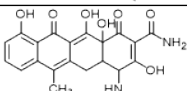
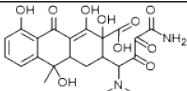
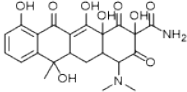
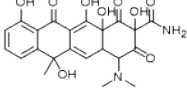
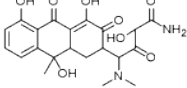
Table S4. Control experiments to prepare CN:Tm nanosheets with different conditions. It is noted that the CN:0.5%Tm sample has the best photocatalytic degradation performance, therefore, the CN:0.5%Tm was chosen to further prepare CN:Tm@UC composites. The abbreviations of the composite samples are shown in Table S5.

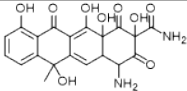
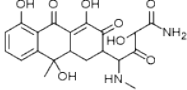
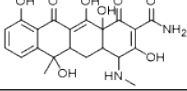
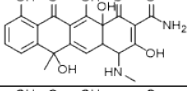
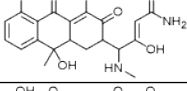
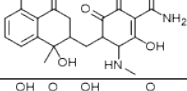
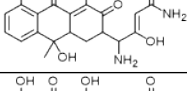
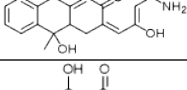
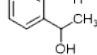
Samples	Melamine	Tm(NO ₃) ₃	First calcination	Second calcination	Condensation reflux
CN	5 g	0 mg	550 °C, 3 h	550 °C, 2 h	120 °C, 2 h
CN:0.1%Tm	5 g	5 mg	550 °C, 3 h	550 °C, 2 h	120 °C, 2 h
CN:0.5%Tm	5 g	25 mg	550 °C, 3 h	550 °C, 2 h	120 °C, 2 h
CN:1%Tm	5 g	50 mg	550 °C, 3 h	550 °C, 2 h	120 °C, 2 h

Table S5. Control experiments to prepare CN:Tm@UC composites with different conditions (the ratio of UC and CN:Tm is the theoretical mass ratio of UC and CN:0.5%Tm), and the TC degradation rate of the corresponding samples after 2 hours of near-infrared light irradiation.

Samples	Ba(NO ₃) ₂ (mmol)	Yb(NO ₃) ₃ (mmol)	Tm(NO ₃) ₃ (mmol)	CN:Tm (g)	Ratio of UC/CNT	Calcined condition	degradation rate
CNT@UC	0.795	0.2	0.005	0.21	1:1	500°C, Air	41.5 %
	0.795	0.2	0.005	0.21	1:1	600°C, Air	38.1 %
	0.795	0.2	0.005	0.21	1:1	700°C, Air	26.2 %
	0.795	0.2	0.005	0.21	1:1	500°C, N ₂	35.2 %
	0.795	0.2	0.005	0.21	1:1	600°C, N ₂	29.3 %
	0.795	0.2	0.005	0.21	1:1	700°C, N ₂	24.5 %
	0.795	0.2	0.005	0.07	3:1	500°C, Air	45.8 %
	0.795	0.2	0.005	0.035	6:1	500°C, Air	55.7 %
	0.795	0.2	0.005	0.023	9:1	500°C, Air	51.0 %
	0.795	0.2	0.005	0.42	1:2	500°C, Air	31.1 %

Table S6. The possible intermediate products of photocatalytic TC degradation by CNT/UC sample under 940 nm light irradiation.

NO.	R.Time	Molecular Formula	Calculated	Observed	Error(ppm)	Structural Formula
1	6.66	C ₂₂ H ₂₄ N ₂ O ₈	445.1605	445.1587	4.04	
2	6.50	C ₂₁ H ₂₂ N ₂ O ₆	399.1551	399.1536	3.76	
3	6.51	C ₂₀ H ₂₀ N ₂ O ₆	385.1394	385.1381	3.38	
4	7.45	C ₂₁ H ₂₀ N ₂ O ₇	413.1343	413.1329	3.39	
5	5.75	C ₂₂ H ₂₄ N ₂ O ₁₀	477.1504	477.1483	4.40	
6	6.22	C ₂₂ H ₂₄ N ₂ O ₉	461.1555	461.1540	3.25	
7	6.94	C ₂₂ H ₂₂ N ₂ O ₉	459.1398	459.1384	3.05	
8	5.65	C ₂₁ H ₂₄ N ₂ O ₈	433.1605	433.1585	4.62	

9	6.68	$C_{20}H_{18}N_2O_9$	431.1085	431.1070	3.48	
10	5.61	$C_{20}H_{22}N_2O_8$	419.1449	419.1427	5.25	
11	6.56	$C_{21}H_{22}N_2O_8$	431.1449	431.1434	3.48	
12	7.34	$C_{21}H_{20}N_2O_8$	429.1292	429.1281	2.56	
13	6.53	$C_{20}H_{22}N_2O_7$	403.1500	403.1478	5.46	
14	6.55	$C_{20}H_{22}N_2O_7$	403.1500	403.1487	3.22	
15	6.88	$C_{19}H_{20}N_2O_7$	389.1343	389.1324	4.88	
16	6.89	$C_{19}H_{17}NO_7$	372.1078	372.1061	4.57	
17	2.25	$C_9H_{10}O_3$	167.0703	167.0728	14.96	

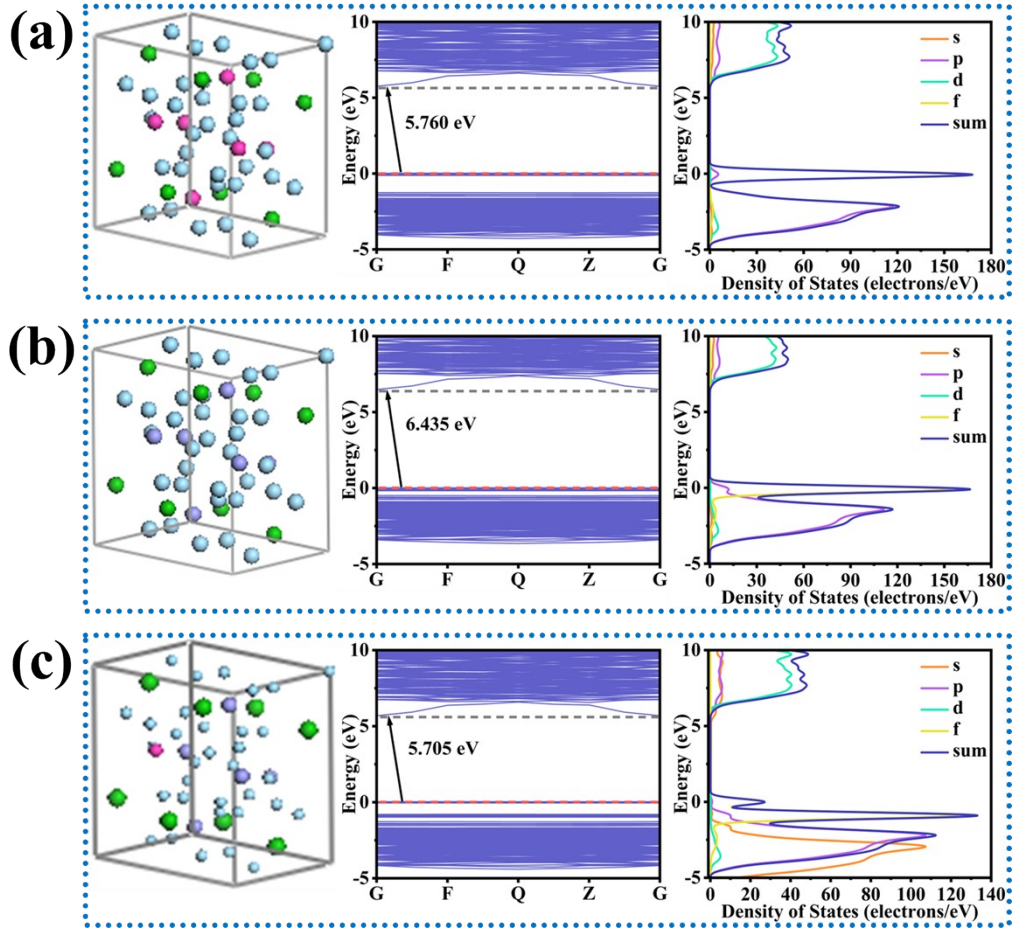


Figure S1. The optimized geometric structures, band-gap structures, and density of states of (a) $\text{Ba}_4\text{Tm}_3\text{F}_{17}$, (b) $\text{Ba}_4\text{Yb}_3\text{F}_{17}$, and (c) $\text{Ba}_4\text{Yb}_3\text{F}_{17}:\text{Tm}$.

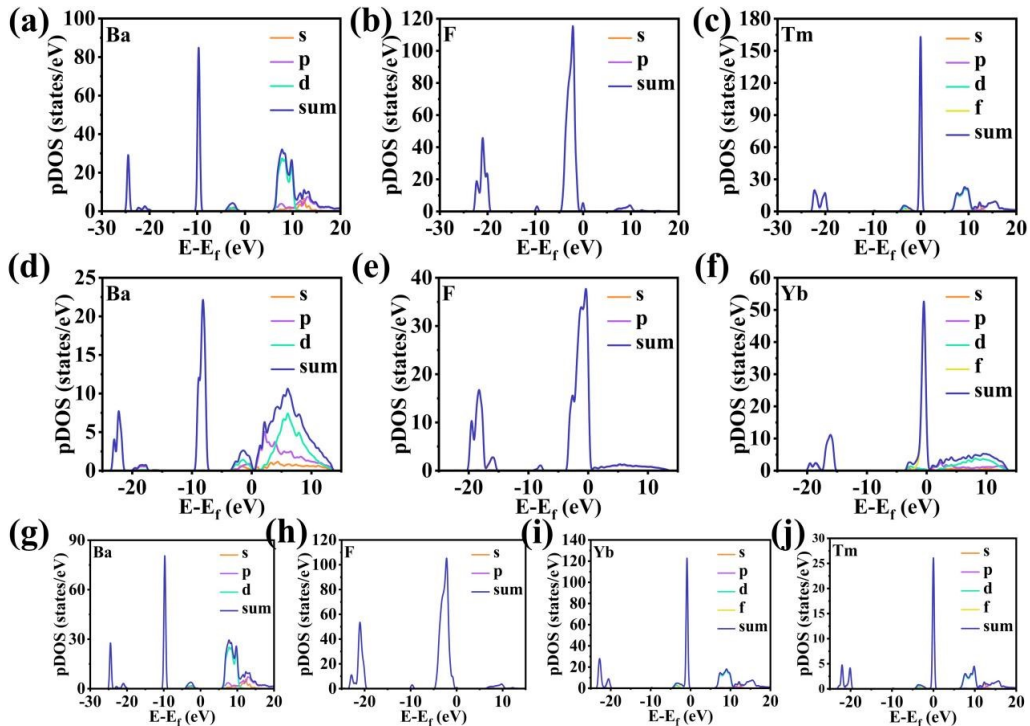


Figure S2. The PDOS of (a-c) $\text{Ba}_4\text{Tm}_3\text{F}_{17}$, (d-f) $\text{Ba}_4\text{Yb}_3\text{F}_{17}$, and (g-j) $\text{Ba}_4\text{Yb}_3\text{F}_{17}:\text{Tm}$.

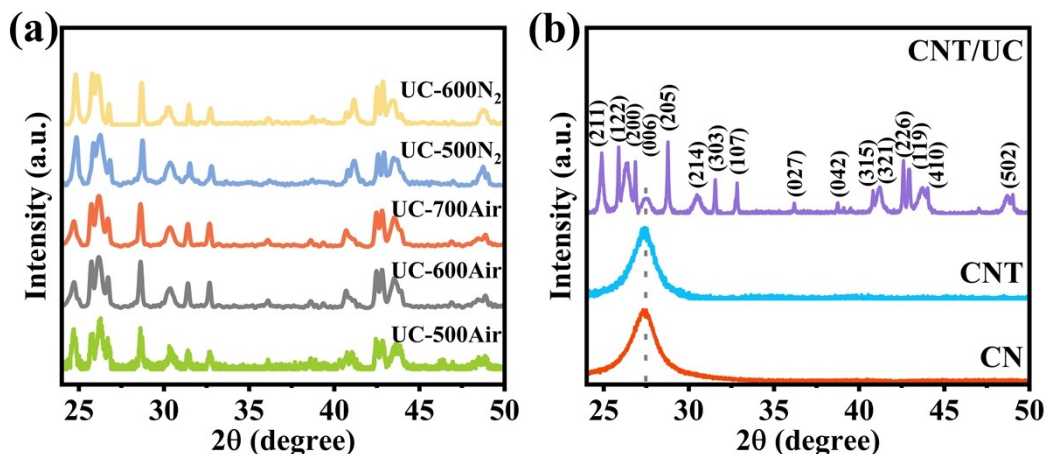


Figure S3. (a) XRD patterns of UC-0.5%Tm samples with different synthesis conditions. (b) XRD patterns (from bottom to top) of CN, CNT, and CNT/UC.

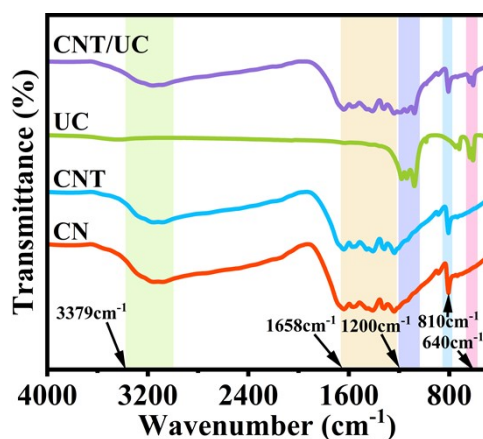


Figure S4. The FT-IR spectra of CN, CNT, UC, and CNT/UC. For CN, CNT, and CNT/UC samples, the peak around 810 cm^{-1} represents the out-of-plane bending mode of the triazine units. The absorption peaks at $1200\sim 1658\text{ cm}^{-1}$ and $3000\sim 3379\text{ cm}^{-1}$ corresponds to the stretching vibrations mode of C-N heterocycles and N-H in bridged or terminal amine groups. The peaks at $602\sim 1190\text{ cm}^{-1}$ may be related to the stretching vibration of O-F-O, O-F, C-F, and Yb-F stretching vibration in $\text{Ba}_4\text{Yb}_3\text{F}_{17}$.

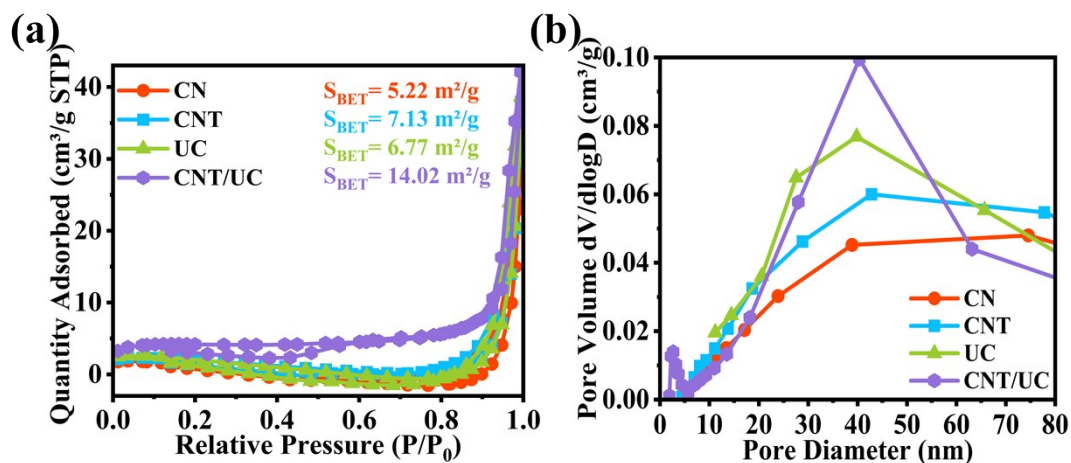


Figure S5. (a) N_2 adsorption-desorption curves and (b) pore size distributions of CN, CNT, UC, and CNT/UC.

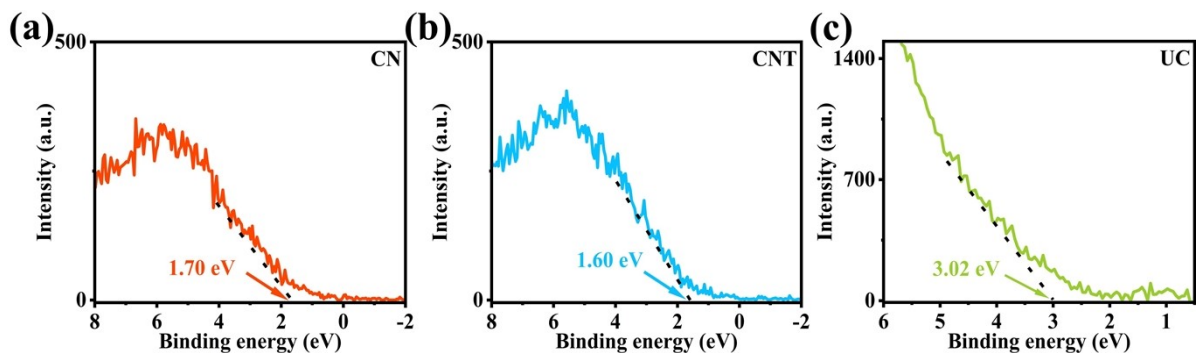


Figure S6. VB-XPS spectra of (a) CN, (b) CNT, and (c) UC nanoparticles.

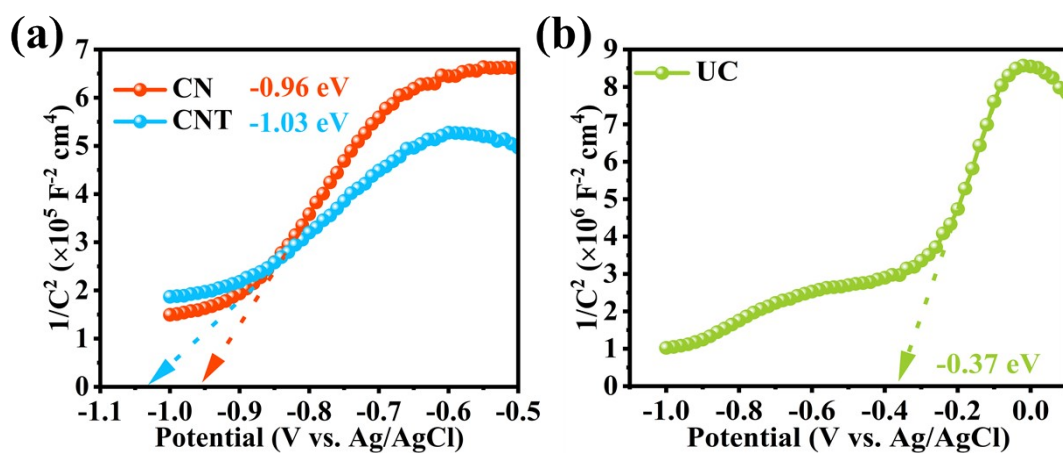


Figure S7. Mott-Schottky plots of CN, CNT, and UC nanoparticles.

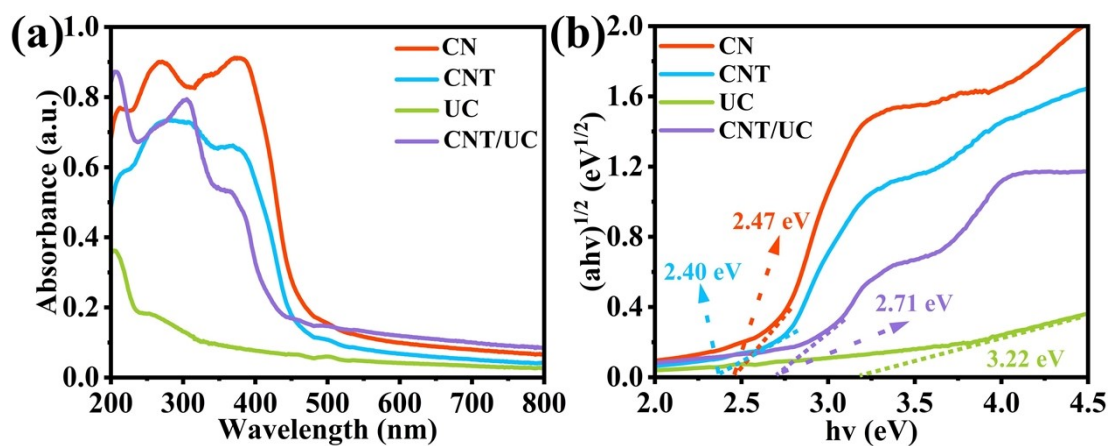


Figure S8. (a) UV-vis DRS and (b) corresponding plots of transformed Kubelka-Munk function versus photon energy of the different samples.

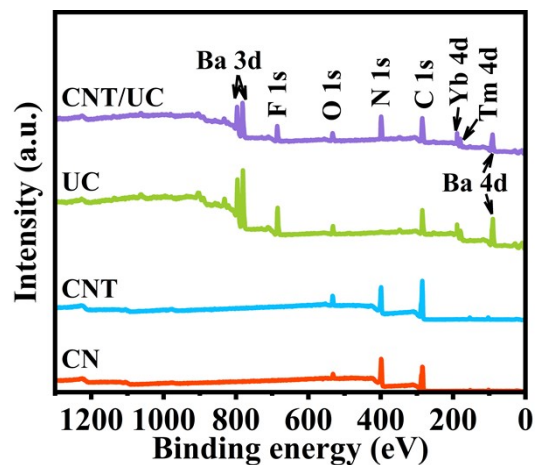


Figure S9. XPS survey spectra of CN, CNT, UC, and CNT/UC.

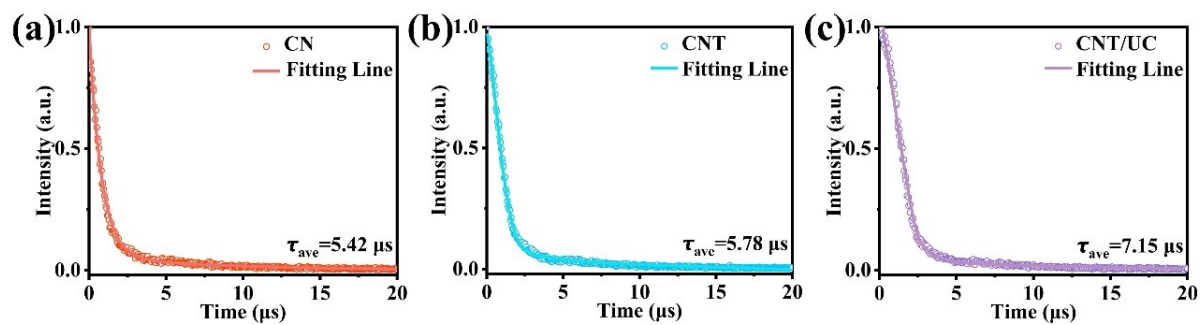


Figure S10. Luminescence decay curves ($\lambda_{\text{ex}} = 290 \text{ nm}$, $\lambda_{\text{em}} = 450 \text{ nm}$) of (a) CN, (b) CNT, and (c) CNT/UC samples.

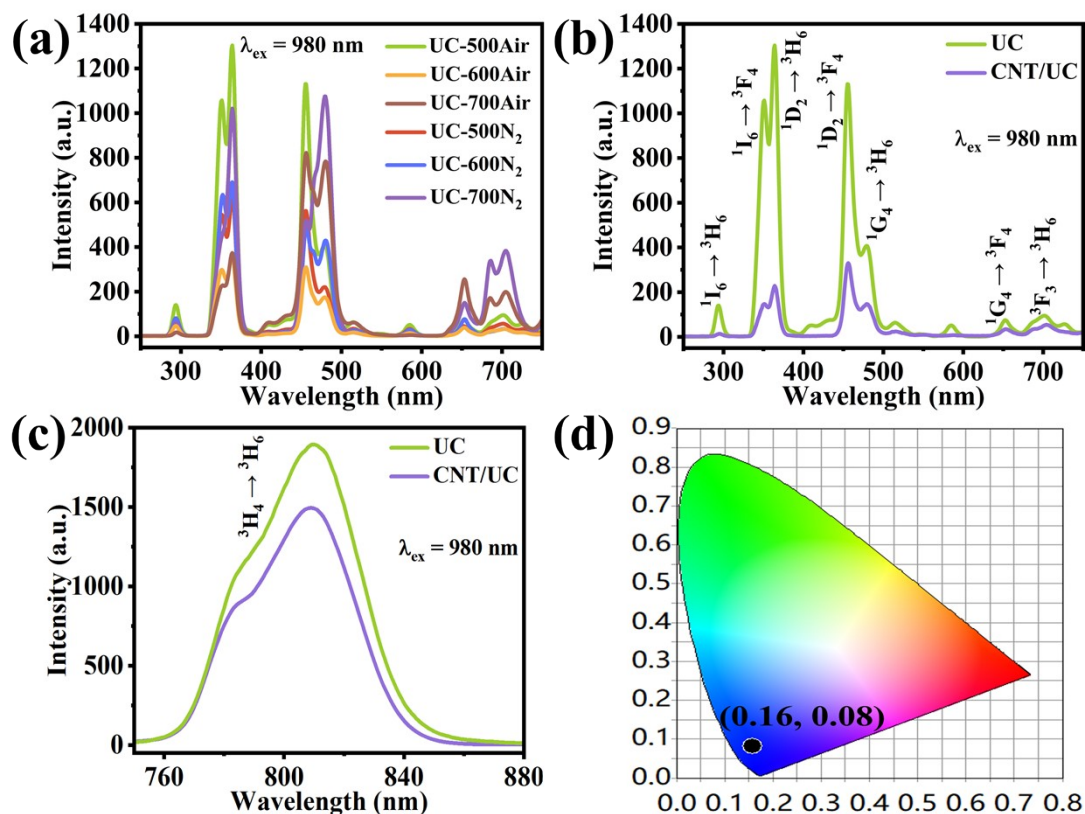


Figure S11. (a) Upconversion luminescence spectra of the UC-0.5%Tm sample calcined at different temperatures in air or nitrogen for 30 minutes. (b, c) Upconversion luminescence spectra of UC and CNT/UC under 980 nm excitation. (d) The CIE chromaticity coordinates for the UC sample under 980 nm excitation.

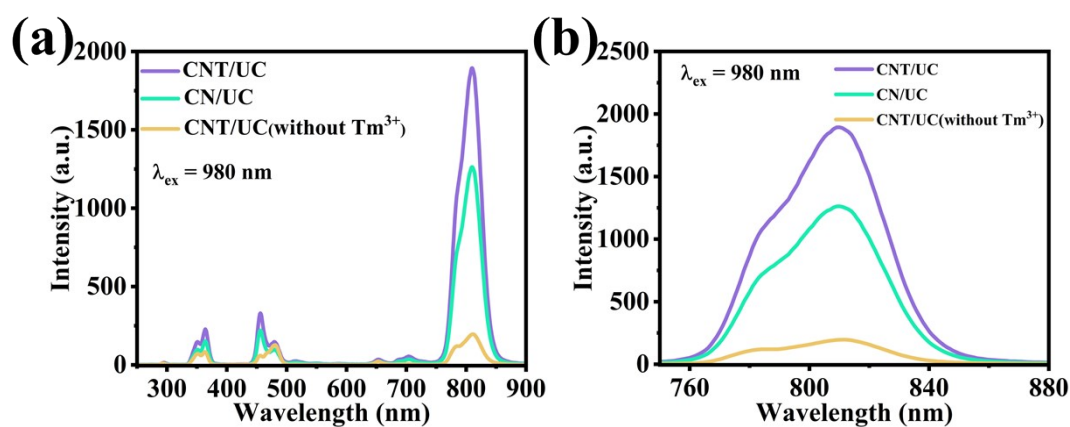


Figure S12. (a) Upconversion luminescence spectra of CNT/UC, CN/UC, and CNT/UC (without Tm^{3+}). (b) Amplified UCL spectra of CNT/UC, CN/UC, and CNT/UC (without Tm^{3+}) samples in the range of 750 to 880 nm.

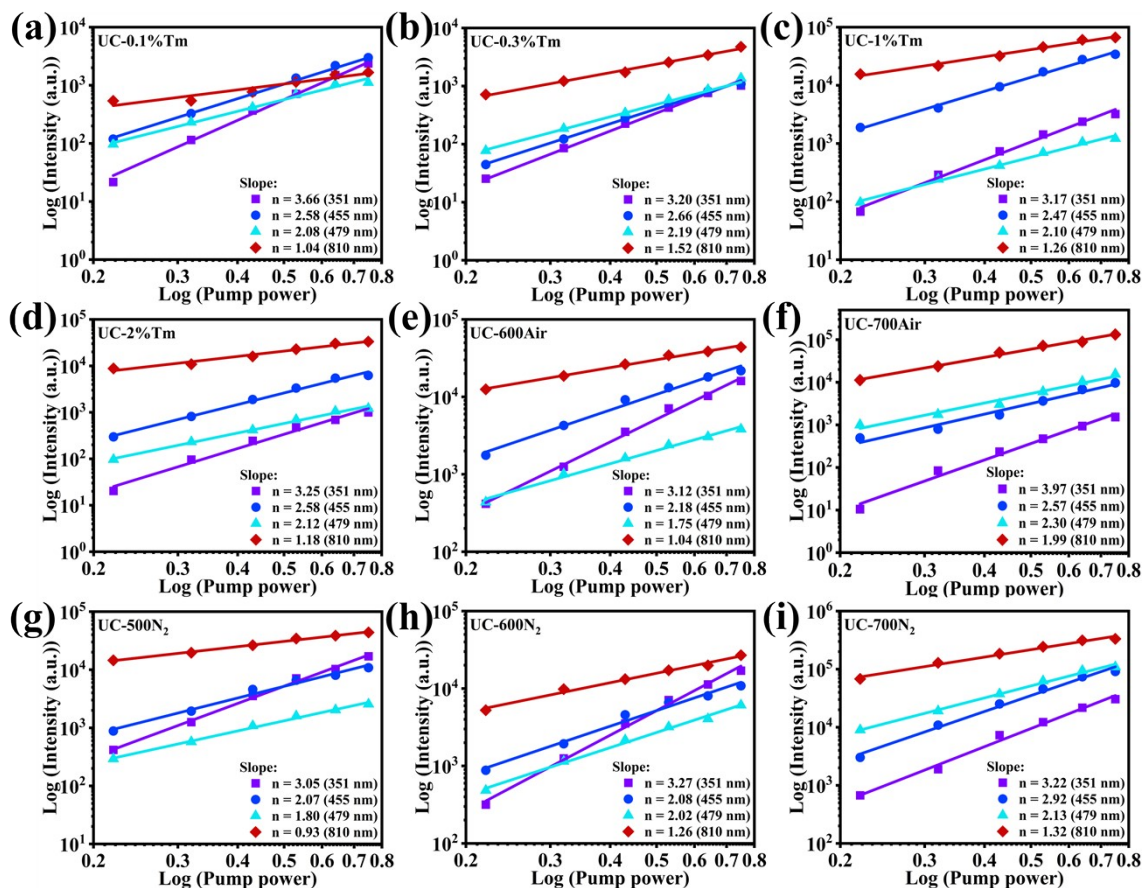


Figure S13. Plots (log-log) of emission intensity versus excitation power in UC nanoparticles with different synthesis conditions (corresponding to Table S1 to Table S3) under 980 nm excitation.

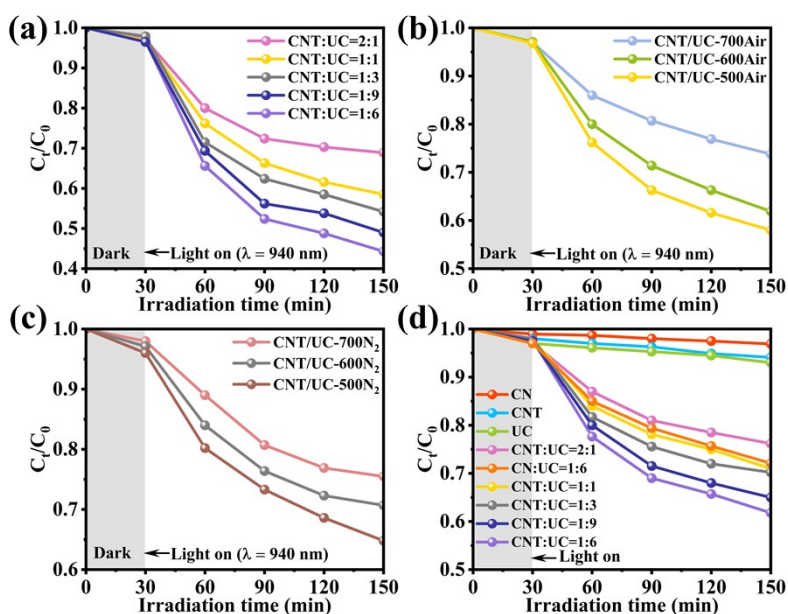


Figure S14. (a) The photocatalytic degradation efficiency of TC by composite materials (500°C, air) with different mass ratios of UC and CN:Tm under 940 nm light irradiation. (b, c) The photocatalytic degradation efficiency of TC by composite samples with different synthesis

conditions (corresponding to Table S5) under NIR light irradiation. (d) The photocatalytic degradation efficiency of CF by various samples under 940 nm light irradiation.

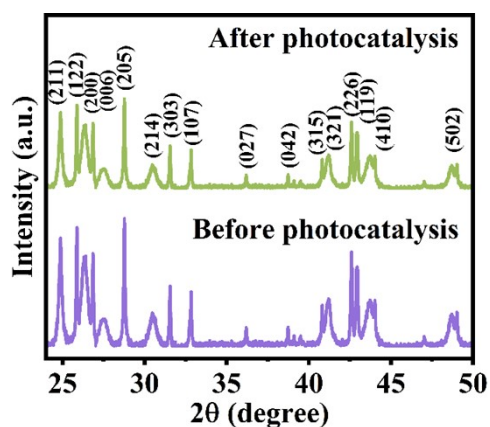


Figure S15. XRD patterns of CNT/UC sample before and after four cycles of photocatalytic reactions.

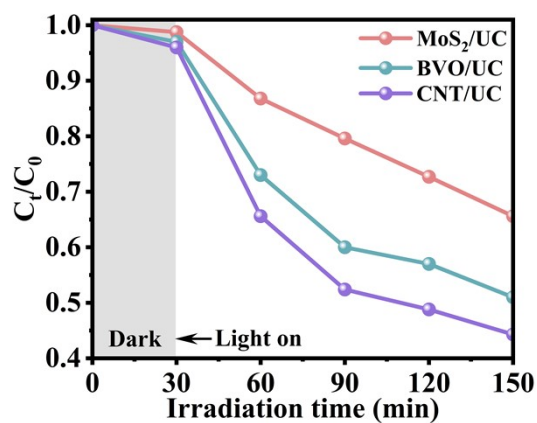


Figure S16. The photocatalytic degradation efficiency of TC over MoS₂/UC, BVO/UC, and CNT/UC samples under 940 nm light irradiation.

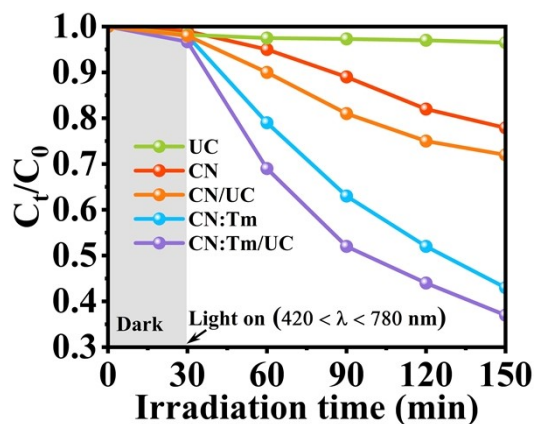


Figure S17. The photocatalytic degradation efficiency of TC under visible light irradiation ($420 < \lambda < 780$ nm).

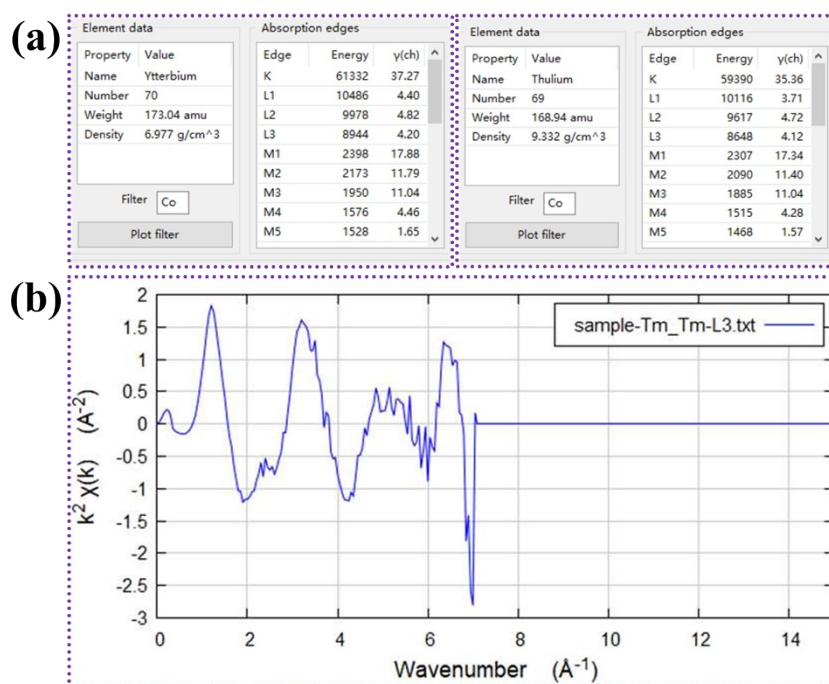


Figure S18. (a) Element data and absorption edges of Tm and Yb elements. (b) FT-EXAFS spectra of CNT/UC sample at Tm L₃-edge in K space.